



Aerodynamic/Structural Optimization of a Training Aircraft Wing

K. Y. Maalawi^{*}, H. M. Negm^{**} and M. M. El Sheikh^{***}

Abstract: This paper presents a coupled aerodynamic/structural optimization model for a light training, low subsonic aircraft wing. Four optimization strategies have been developed and tested. The first was based on minimization of the total weight of the main wing structure subject to strength, stiffness and aeroelastic constraints. The second strategy considered maximization of the critical flight speed at which divergence occurs, while the third one focused on minimization of the wing drag/lift ratio as a measure of improving aerodynamic efficiency without violating structural weight requirements. The last strategy was based on minimization of the power consumption, which has worked very well and shown balanced improvements in both the aerodynamic and structural efficiencies of the wing under the imposed design constraints. The aerodynamic variables are chosen to be the wing aspect and chord taper ratios, while the structural variables encompassed spar locations, spar flange cross-sectional areas, shear webs and covering skin thicknesses of the main wing box section. The optimization problem has been formulated as a nonlinear mathematical programming problem solved by invoking the MATLAB optimization Toolbox routines, which implements the method of feasible directions. Structural, aerodynamic and aeroelastic analyses assumed slender one-dimensional configuration. It makes use of the quasi-steady strip theory in evaluating aerodynamic loads and the classical engineering theories of bending and torsion in calculating stresses and deformations. Results have shown that the approach implemented in this study can be efficient in producing improved designs in a reasonable computer time. The proposed model has succeeded in arriving at the optimum solutions showing significant improvements in the needed design goals as compared with a baseline wing design.

Keywords: Wing design, Structural Optimization, Aerodynamics, Aeroelasticity.

1. Introduction

Design optimization has been gaining increasing attention in recent years for its acknowledged contributions made to design enhancement, especially in early stages of product development. Pioneer applications can be found in the aerospace industry where light weight structural components are required for either cost reduction or payload increase.

^{*} Associate Professor, National Research Centre, Dokki, Cairo, Egypt /
NRC.AERO@Gmail.Com

^{**} Professor, Aerospace Engineering, Faculty of Engineering, Cairo University, Giza, Egypt.

^{***} Egyptian Armed Forces, Egypt/ mabokhers@yahoo.com.

Ashley [1] presented a brief for the potential applications of optimization in the field of aeronautical engineering, where several design aspects concerning both aerodynamic and structural optimization were identified and discussed. Edwin [2] considered optimization of the Grumman X-29, forward swept wing with the objective of minimizing structural weight under constraints imposed on strength and divergence velocity. Grossman et al. [3] investigated the interaction of aerodynamic and structural optimization for a sailplane wing via a sequential design procedure. The number of the selected design variables ranged between 25-35 variables and the chosen criteria of the optimal design problem included maximization of aerodynamic performance and minimization of structural weight under aeroelastic constraints. In the context of aeroelastic optimization of aircraft structures, Butler et al. [4] calculated the minimal mass design of high aspect ratio composite wing under the condition that both divergence and flutter speeds not to exceed permissible upper limiting values. The wing was modeled as a series of box beams whilst aeroelastic loads were based on the aerodynamic strip theory. Design variables encompassed engine position, spars locations as well as laminate ply thickness variation. Peter J. et al. [5] presented a combined aerodynamic and structural optimization model of a high-speed civil transport wing. Design objectives included minimum aerodynamic drag and structural weight subjected to constraints imposed on torsional divergence, strength, and buckling. Other research studies in the field of aerospace industry attempt in the direction of aircraft Multidisciplinary Design Optimization (*MDO*). Negm and Maalawi [6] formulated a global objective function for design optimization of civilian transport airplanes. They considered a host of design objectives and constraints in a broad sense, where several optimization strategies were tried out, including airplane weight, structural safety, ride comfort and cost. Livine et al. [7] optimized a composite wing structure, considering both aerodynamic and structural efficiencies in the model formulation. The aerodynamic efficiency was measured by the minimum drag requirements while structural efficiency was measured by minimum structural weight under strength and stiffness constraints. The development and use of the Automated Structural Optimization System (*ASTROS*) with wing structural design in multidisciplinary environment were discussed by Neill et al. [8], who implemented the feasible directions algorithm with sensitivity analysis and constraint approximations. Papila et al. [9] considered different optimization strategies by investigating the induced drag penalty associated with flight conditions having lower lift coefficient than the one associated with the design flight conditions. Their wing structural model consisted of main box section and fifteen equally spaced ribs. Other recent studies by Librescu and Maalawi [10, 11] dealt with optimization of composite wings having spanwise grading in either material or shear wall thickness. The objective function was measured by maximization of the divergence speed while maintaining the total structural weight at a value equal to that of a baseline design. It was shown that global optimality solutions can be achieved for a variety of wing configurations.

The present work aims at the development of a model for design optimization of a low subsonic, light training airplane wing. The selected design variables represent aerodynamic as well as structural parameters of the system. The study implements the Matlab optimization toolbox routines, which interact with the developed wing structural, aeroelastic and aerodynamic analyses routines, in order to find the needed optimum solutions for various flight conditions. The general aspects of wing design optimization, including the main design objectives, variables and constraints are outlined and discussed in detail. Finally, the optimum trends for good wing designs at different flight specifications are discussed with the relevant concluding remarks for future extension of this research work.

2. Main Aspects of Wing Design Optimization

An airplane wing is a complex structural system with numerous variables and constraints. It contains thousands of structural components, ranging from small bolts and rivets to large, heavyweight skin panels and spars. Therefore, creation of a detailed wing model incorporating, simultaneously, all the wing features is virtually impossible. Thus, researchers and engineers rely on simplified models which provide a fairly accurate approximation of the real wing structure behavior. In this section we shall apply the underlying concepts of optimization theory to the design of a conventional airplane wing structure. The relevant design objectives, constraints and variables are identified and discussed in detail.

2.1 Wing design objectives

The wing is the main lifting surface in an aircraft. There are two rather conflicting goals for its design, namely, the improvement of structural and aerodynamic efficiencies. In the present simplified formulation the structural efficiency will be improved through weight reduction and maximization of the overall stiffness level while considering strength and stability requirements as design constraints. The torsional stiffness of the wing can be enhanced by maximization of the critical flight speed (V_{Div}) at which divergence occurs. On the other hand, the improvement of the lift and drag characteristics of a wing further some other design objectives of the whole airplane like long range, low power consumption and operating cost. Minimization of the drag / lift ratio (D_L) is an aerodynamic design criterion which is bound to produce good wing configuration. It can lead to a substantial improvement in the airplane performance as well as the overall operational economy. The rate of fuel consumption will be decreased and the flight duration will be increased. Minimization of the power required to maintain flight can be a better and straighter forward criterion than minimizing the (Drag/lift) ratio. The power depends upon the airplane resistance forces (drag) and the flight speed. However, in the present simplified model, the airplane speed, the flight altitude, and the load factor are all preassigned. Therefore, one may suggest minimization of the product ($F_w \cdot D_L$) as a representative of the of the power consumption, where F_w is the weight of the main wing structure. Final judgment on the proper selection of the objective function has to wait for actual computer implementation of the different models outlined above.

2.2 Wing design variables

The wing design variables include layout parameters as well as cross-sectional variables. The most important variables of a wing structure are classified in the following:

2.2.1 Wing layout

- a- The planform which is defined by the wing aspect ratio, chord taper ratio and the sweep angle measured to the quarter-chord line.
- b- The wing section geometry, which may be described by the NACA-series airfoil number signifying certain thickness and camber distributions.
- c- The spanwise rigid twist distribution.
- d- The dihedral angle.

2.2.2 Wing cross-sectional and spanwise variables

- a- The type of wing cross- section (e.g. concentrated or distributed flange type).
- b- The type, number, location and dimensions of spars, stringers, ribs and covering skin.

- c- Spar flange area, shear web and skin thicknesses distributions along wing span.
- d- Types of materials of construction.

2.3 Design constraints

A design that meets all the requirements placed on it is called a feasible design. In the present simplified wing model the behavioral constraints are:

2.3.1 Strength requirements

No yielding under shear or bending.
No web buckling under inplane shear.

2.3.2 Stiffness considerations

Prevention of wing divergence.
Elimination of wing excessive deflections.

2.3.3 Performance requirements

These include the maximum total lift coefficient requirement and the maximum available engine horsepower.

Other side constraints are imposed on the values of the design variables for geometrical or logical reasons. They include:

- Non-negativity constraints on certain variables to avoid obtaining negative dimensions in the solution.
- Limitations on spar locations to make room for flaps, ailerons, etc.....
- Upper and lower limits on the wing aspect and chord taper ratios to avoid having odd-shaped configuration in the resulting optimal solution.

3. Aerodynamic/Structural Analysis

3.1 Basic Assumptions

We consider here the case of symmetric flight condition at a given speed, altitude and load factor. The speed will be assumed to be low subsonic. The critical loading condition to be considered in sizing the structural elements of the wing is taken to be the flight case of pullout from a dive. The wing will be assumed to have trapezoidal, unswept planform. Furthermore, assuming the wing to be slender with no major cutouts, the engineering beam theory can be employed and the state of deformation can be completely described in terms of one space coordinate i.e. y-coordinate, as shown in Fig. 1.

3.2 Governing Differential Equations

The wing differential equations of equilibrium in bending and torsion are respectively given by [12]:

$$\text{Bending: } \frac{\partial^2}{\partial y^2} \left[EI(y) \frac{\partial^2 w(y)}{\partial y^2} \right] = F(y) \quad (1)$$

$$\text{Torsion : } \frac{\partial}{\partial y} \left[GJ(y) \frac{\partial \theta(y)}{\partial y} \right] = T(y) \quad (2)$$

where EI is the flexural rigidity about the centroidal x-axis, $w(y)$ upward bending deflection, $F(y)$ upward load distribution, GJ torsional rigidity about the shear center, θ nose up twisting angle and $T(y)$ is the distribution of the nose-up twisting moment. The wing reference axes are shown in Fig. 1. The associated boundary conditions are described by:

$$w, w', \theta = 0 \text{ at } y = 0 \quad \text{and} \quad EIw'', (EIw'')', (GJ\theta')' = 0 \text{ at } y = b \quad (3)$$

where primes denote differentiation with respect to y and b is the wing semispan. Utilizing the influence function concept [12] the solution of Eqs.(1) and (2) can be cast as follows:

$$w(y) = \int_0^b C^{zz}(y, \eta).F(\eta) d\eta; \quad \theta(y) = \int_0^b C^{\theta\theta}(y, \eta).T(\eta) d\eta \quad (4)$$

where $C^{zz}(y, \eta)$ and $C^{\theta\theta}(y, \eta)$ are called the bending and torsional influence functions, respectively. For a symmetric flight condition the upward force and the twisting moment about the wing elastic axis are given by:

$$\text{Upward Force: } F(y) = qc(y)C_L(y) - N_z mg(y) \quad (5)$$

$$\text{Twisting moment: } T(y) = qc(y)C_L(y)e(y) + qc^2(y)C_{m.a.c.}(y) - N_z mg(y).d(y) \quad (6)$$

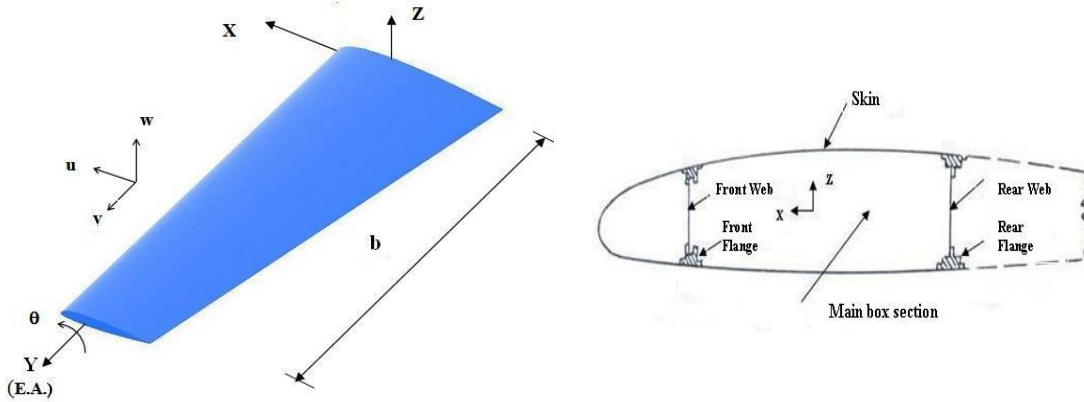


Fig. 1. Wing Layout and Cross-Sectional Configuration.

where q is the dynamic pressure ($=\rho_{air}V^2/2$), C airfoil chord, C_L lift coefficient, $C_{m.a.c.}$ pitching moment coefficient, N_z vertical load factor, $mg(y)$ spanwise distribution of the wing weight per unit length, $e(y)$ distance between aerodynamic center and shear center and $d(y)$ distance between the shear center and gravity center. The total angle of attack $\alpha(y)$ is composed of two parts: the rigid angle α^r and the elastic twist θ . The rigid angle is composed of two parts: the setting angle α_0 at the wing root and the rigid twist $\alpha_t(y)$.

$$\alpha = \alpha^r + \theta; \quad \alpha^r = \alpha_0 + \alpha_t \quad (7)$$

The local lift coefficient c_L is split into a rigid part c_L^r corresponding to α^r and an elastic part c_L^e corresponding to θ :

$$c_L = c_L^r + c_L^e \quad (8)$$

The elastic twisting angle is:

$$\theta(y) = q \int_0^b C^{\theta\theta}(y, \eta) \cdot c \cdot c_L^e \cdot e \cdot d\eta + f(y) \quad (9a)$$

where $f(y)$ is a disturbance function defined as:

$$f(y) = \int_0^b C^{\theta\theta}(y, \eta) [q \cdot c \cdot c_L^r \cdot e + q \cdot c^2 \cdot c_{mac} - N_z \cdot mg \cdot d] d\eta \quad (9b)$$

3.3 Multhopp discretization

The infinite-degree of freedom system will be approximated by a finite, discrete system. All functions will be discretized using the so-called Multhopp stations [12]. Thus the influence functions in Eq. (4) are expressed as:

$$C_{ij}^{zz} = \int_0^{y_i} \frac{y_i(y_i - y)(y_j - y)}{EI(y)} dy, \quad y_i \leq y_j \quad ; \quad C_{ij}^{\theta\theta} = \int_0^{y_i} \frac{1}{GJ(y)} dy, \quad y_i \leq y_j \quad (10)$$

where $i, j = 1, 2, \dots, n_r$ and n_r is the total number of the wing semispan Multhopp stations. Accordingly, Eq. (9) takes the following matrix form:

$$\{\theta\} = q[E]\{c c_L^e\} + \{f\} \quad (11a)$$

$$\{f\} = q[E]\{c c_L^r\} + q[D]\{c_{mac}\} - N_z[G]\{mg\} \quad (11b)$$

The individual matrices are defined as follows:

$$[E] = [C^{\theta\theta}] \begin{bmatrix} e \\ \bar{w} \end{bmatrix} ; \quad [D] = [C^{\theta\theta}] \begin{bmatrix} c^2 \\ \bar{w} \end{bmatrix} ; \quad [G] = [C^{\theta\theta}] \begin{bmatrix} d \\ \bar{w} \end{bmatrix} \quad (12)$$

The angle of attack α_0 corresponding to prescribed values for N_z and q is calculated from [12]

$$\alpha_0 = \frac{1}{[R][1]} [N_z(W_{a/c}/2 + [R][G]\{mg\}) - q[R][D]\{c_{mac}\} - [R]\{\alpha_t\}] \quad (13a)$$

$$\text{Where } [R] = q[1] \begin{bmatrix} \bar{w} \end{bmatrix} [B]^{-1} \quad \text{and} \quad [B] = [A^s] - q[E] \quad (13b)$$

$W_{a/c}$ is the total aircraft weight and $\begin{bmatrix} \bar{w} \end{bmatrix}$ is a diagonal matrix containing the weighting factors of Multhopp's integration formula which is given by:

$$\bar{w}_i = \frac{\pi b}{2n_r} \sin \phi_i, \quad \bar{w}_{nr} = \pi b / 4n_r, \quad \phi_i = i \cdot \frac{\pi}{2n_r} \quad i = 1, 2, \dots, n_r \quad (14)$$

Working with the aerodynamic strip theory corrected for three-dimensional flow, the elements of the diagonal symmetric aerodynamic matrix $[A^s]$ can be determined from $A^s_{ii} = 1/a_i c_i$ where a_i is the airfoil corrected lift curve slope [14] at the i -th station. Thus using α_0 and $[B]$, the lift distribution can be calculated from:

$$q\{c_{c_L}\} = q[B]^{-1}\{\alpha^r\} + q[D]\{c_{mac}\} - N_z[G]\{mg\} \quad (15)$$

The wing total drag force can be calculated from the relation $D = N_z W_{A/C} D_L$, where D_L is the (drag/lift) - ratio given by:

$$D_L = \frac{C_D}{C_L} = \left(\frac{C_{D_0}}{C_L} + \frac{C_L}{\pi f_1 AR} \right) \quad (16)$$

C_L is the wing total lift coefficient, C_{D_0} the wing profile drag coefficient and $f_1(\lambda, AR)$ is the span efficiency factor function [14] depends upon the aspect ratio AR and chord taper ratio λ .

3.4 Wing Divergence

Divergence is static wing torsion instability that occurs at a certain dynamic pressure q_D , which is determined by consideration of the non-trivial solution of the matrix equation:

$$([P] - \frac{1}{q}[I])\{c c_L^e\} = \{0\} \quad ; \quad [P] = [A^s]^{-1}[E] \quad (17)$$

The largest eigenvalue corresponds to the smallest dynamic pressure q_D at which divergence occurs. The divergence speed is then given by:

$$V_D = \sqrt{2q_D / \rho_{air}} \quad (18)$$

3.5 Wing Deformations

The wing bending and torsion displacements are calculated from:

$$\{w\} = [C^{zz}] \left[\begin{array}{c} \backslash \\ w \backslash \end{array} \right] \{F\} \quad ; \quad \{\theta\} = [c^{\theta\theta}] \left[\begin{array}{c} \backslash \\ w \backslash \end{array} \right] \{T\} \quad (19)$$

where the normal force $\{F\}$ and the twisting torque $\{T\}$ can be calculated from Eqs. (5) & (6).

3.6 Wing Stress Analysis

Having determined the aerodynamic load distribution, the bending and shear stresses can be calculated. Homogeneous material and linear-elastic behavior are assumed. The skin covering and shear webs will be considered ineffective in carrying bending loads. The bending stress σ_{ij} in the i -th spar flange at the j -th station is calculated using the engineering beam theory of bending [15]. The shear flow due to bending and torsion will be calculated separately and then added together. The shear stress τ_{ij} in any panel is then calculated by dividing the local shear flow by the local thickness. The buckling shear stress $(\tau_{cr})_{ij}$ of the i -th internal web at the j -th wing station is calculated from [15]

$$(\tau_{cr})_{ij} = \frac{k_s \pi^2 E}{12(1-\nu^2)} \left(\frac{t_w}{r_s} \right)_{ij}^2 \quad (20)$$

where k_s = buckling coefficient depending upon the web panel aspect ratio, r_s = web-stiffener spacing, t_w =web thickness, E =modulus of elasticity and ν = Poisson's ratio of sheet material.

4. Optimization Analysis

MATLAB is a powerful tool for advanced mathematics, engineering and science research [16]. Its optimization toolbox includes many routines for different types of optimization encompassing both unconstrained and constrained minimization algorithms [13]. One of the useful *MATLAB* routines is named “*fmincon*” which attempts to find the constrained minimum of an objective function $F(\underline{X})$ of a vector \underline{X} of design variables, subject to certain number of constraints $G_j(\underline{X}) \leq 0$, $j=1,2,\dots,m$. This is generally referred to as constrained nonlinear optimization or nonlinear programming. The “*fmincon*” routine implements the method of feasible directions in finding the required constrained minimum, where the search direction \underline{S}_j must satisfy the two conditions $\underline{S}_j \cdot \underline{\nabla} F < 0$ and $\underline{S}_j \cdot \underline{\nabla} G_j < 0$, where $\underline{\nabla} F$ and $\underline{\nabla} G_j$ are the gradient vectors of the objective and constraint functions, respectively. For checking the constrained minima, the Kuhn-Tucker test [13, 16] is applied at the design point \underline{X}_D , which lies on one or more set of active constraints.

4.1 Design Variables \underline{X}

The selected design variables of the present simplified wing model are defined in the following:

- a- Layout variables (2 variables)
 - 1- Wing aspect ratio AR .
 - 2- Wing chord taper ratio λ .
- b- Cross-sectional variables

Front and rear spar locations e_1 and e_2 (2 variables).

These locations are expressed in percentage of the wing chord from the leading edge.

Front and rear spar flange cross-sectional areas at wing root and tip (4 variables).

Front and rear shear web thicknesses at wing root and tip (4 variables).

Covering skin thickness at wing root and tip (2 variables).

The spar compression flanges are considered to have the same cross sectional area as the tension flange. Both are assumed to have parabolic area variation with span. The shear webs and covering skin thicknesses are assumed to vary linearly with span. Therefore, the total number of the selected design variables is 14.

4.2 Design Constraints $G_j(\underline{X})$

The imposed design constraints are defined in the followings:

Yielding prevention: In bending: $\max 1 \sigma_{ij} \leq \sigma_{allow}$, $i=1, 2$; $j=1,2,\dots,6$

In shear : $\max 1 \tau_{ij} \leq \tau_{allow}$ $i=1,2,3$; $j=1,2,\dots,6$

Web buckling prevention: $|\tau_{ij}| \leq (\tau_{cr})_{ij}$, $i=1,2,3$; $j=1,2,\dots,6$

where $i=1$ refers to front spar, $i=2$ to rear spar and $i=3$ to covering skin. The index (j) refers to Multhopp stations along the wing semi-span.

Prevention of wing divergence $V_{max.} \leq (V_{Div}/1.5)$

Maximum deflection constraint $\delta_{max} \leq \delta_{allow}$

Horsepower limit $HP_{req} \leq HP_{av}$

where HP_{req} represents the required horsepower to maintain flight and HP_{av} is the available horsepower from the airplane engines.

Non-negativity constraints

Spar flange cross-sectional areas: $A_{ij} \geq 0 \quad i=1,2; \quad j=1,6$

Shear webs and skin thicknesses: $t_{wij} \geq 0 \quad i=1,2,3; \quad j=1,6$

Limitations on the spar's locations

Front spar: $e_1 \geq e_{1d}$

Rear spar: $e_2 \leq e_f$

where e_{1d} is the leading edge de-icer distance being equal to 10% of the chord and e_f is the flap location being equal to 65% of the chord.

Limitations on the wing aspect and taper ratios $6 \leq AR \leq 10$ and $0.3 \leq \lambda \leq 1$

4.3 Objective function $F(\underline{X})$

Four design objectives are considered in the present model implementation, including weight minimization of the main wing box section (F_w), maximization of the divergence speed (V_{Div}), minimization of the drag/lift ratio (D_L) and minimization of the power consumption represented by the multiplication ($F_w * D_L$), (refer to section 2.1).

5. A Case Study: Optimization of a Trainer Wing Structure

The developed optimization model will be applied to a wing of a low subsonic, light training airplane; namely, the AEIO-360A airplane for ground observations and coast patrol. It is a single 200hp-engine propeller driven airplane with maximum level speed of 78 m/s at sea level and maximum takeoff weight of 1297 kgs. The wing is cantilevered to the fuselage of whole metal structure except the control surfaces are from glass fiber laminated composites.

5.1 Definition of the baseline design and preassigned parameters

The basic technical data and the associated preassigned parameters of the wing baseline design are described as follows: surface area, $S_w = 11.8 m^2$, wing span ($2b$) = 9.60 m, rigid twist, $\alpha_{i,j} = \alpha_{i,max} * Y_j/b$, $j=1,2, \dots, 6$, where $\alpha_{i,max}$ is the maximum twist at the wing tip. The main wing box section is chosen to be of concentrated flange type with two spars, front and rear ($n_s=2$). The internal wing ribs are spaced at 3% of the wing semispan. All sections composing the wing have the same airfoil type of NACA five-digit 230XX series. The aerodynamic characteristics of the airfoils, used in the present case study, are obtained from reference [14]. The material of construction of spars, web, and skin is chosen to be 7075 Aluminum alloy [15] which has the following properties: yield normal strength = $4 \times 10^8 N/m^2$, yield shear strength = $1.6 \times 10^8 N/m^2$, elastic moduli $E = 7 \times 10^{10} N/m^2$ and $G = 2.65 \times 10^{10} N/m^2$, Poisson's ratio $\nu = 0.32$ and mass density = $2800 Kg/m^3$. The factor of safety shall be taken 1.5. In addition to

the above preassigned parameters, the fixed average weight of the non-structural and the other structural components in the wing per unit area is taken equal to that of the baseline design, *i.e.* 250 N/m^2 . The baseline design variables are listed in Table 1.

Table 1 Baseline Design of the Wing

<i>Design variable</i>	Numerical value/ spanwise distributions
Aspect ratio (AR)	7.81
Taper ratio (λ)	0.5375
Front spar location (e_1)	0.25
Rear spar location (e_2)	0.60
Shear web thickness distributions $t_w(\hat{y})$	Skin: $1.25(1-0.496\hat{y})$ mms * Front & Rear spars: 1.5 mms $0 \leq \hat{y} \leq 1$
Flange area distribution $A_i(\hat{y}), i=1,2$	Front & Rear spars: $15(1-0.4\hat{y}^2)$ cm^2

* \hat{y} is a dimensionless coordinate: $\hat{y} = y/b$; where b is the wing semispan.

5.2 Normalized Quantities

The various structural and aerodynamic quantities are normalized by referring them to the allowable values pertinent to the wing baseline design as given in Table 2. This enables us to simplify analysis and discussion of the optimization results.

Table 2 Definition of Normalized Quantities

Quantity	Notation (units)	Normalization
Shear web thickness	t_w (mms)	$\hat{t}_w = t_w/1.5$
Covering skin thickness	t_s (mms)	$\hat{t}_s = t_s/1.25$
Spar flange area	A_i (cm^2)	$\hat{A}_i = A_i/15$
Bending stress	σ (MPa)	$\hat{\sigma} = \sigma/266.65$
Shear stress	τ (MPa)	$\hat{\tau} = \tau/106.65$
Structural mass	M (kgs)	$\hat{M} = M/97.8$
Divergence speed	V_D (m/s)	$\hat{V}_D = V_D/529.7$
(Drag/Lift) ratio	D_L	$\hat{D}_L = D_L/0.056$
Power consumption	P_r	$\hat{P}_r = P_r/5.5$

5.3 Computer Experimentation on the Effect of the Different Strategies

In this section we shall attempt to test the effect of each of the previously defined objective functions by comprehensive computer implementation. We shall designate the various optimization strategies by the index notations defined in Table 3.

Table 3 Index Notations for the Different Optimization Strategies

Optimization Strategy	Index
Baseline design	0
Min. Structural weight	I
Max. Divergence speed	II
Min. (Drag/Lift) ratio	III
Min. power consumption	IV

A graphical representation of the attained optimization gain in each case, as measured from the baseline design, is shown in Fig.2. The diving speed, load factor and flight altitude are kept at the design values 108.0 m/s, 6.0 and 3.0 Km, respectively. It is seen that all gains start at zero values corresponding to the baseline design. Considering the first strategy, it is seen that mass saving reached a value of 45% as measured from the baseline design. However, both of the torsional stability and (drag/lift) ratio were slightly degraded by 12% and 20%, respectively, but the final optimal solution was still conservative. The power consumption has also reduced considerably by about 34%, indicating significant improvement as compared to the baseline design. The second strategy has resulted in a sharp increase in the torsional stability by 120%, but, in the expense of degrading the (drag/lift) ratio and power consumption by about 25% as indicated in Fig.2. The mass constraint is always active in this category. Such jump in the divergence speed can be expected due to the fact that it is too sensitive to the location of the shear center, which when approaches the aerodynamic center can result in a great increase in the divergence speed of the wing. Examining the third optimization strategy, it is observed that the wing aerodynamic efficiency has enhanced by 22% higher than that of the baseline design. However, considerable degradation occurred in the torsional stability, which reached a value of 40% below the baseline design, and the mass constraint became also active as occurred in the second strategy.

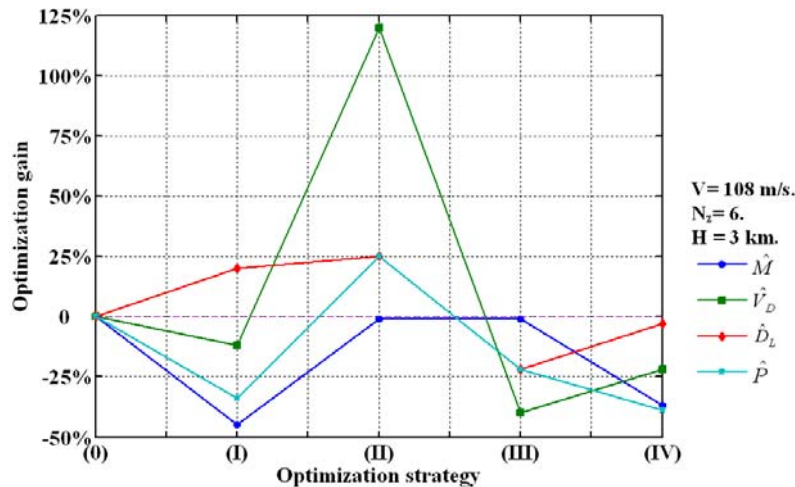


Fig. 2. Attained Optimization Gain for the Different Strategies.

5.4 Optimal Solutions Based on the Minimal Power Criterion

From the performed computer experimentations, it becomes evident that the minimal power consumption has been quite successful and shown balanced improvement in both the structural and aerodynamic efficiencies. The introduction of the (drag/lift) ratio caused an improvement in the aerodynamic efficiency without being overwhelmed by the structural efficiency. The aspect ratio was no longer forced to sink to its lower limiting value as occurred in the other optimization strategies. This model gives the best enhancement of the wing structural weight as well as the (drag/lift) ratio. In the following several optimum patterns of the wing will be presented for different values of the flight design parameters including the maximum design load factor and the maximum diving speed as well.

5.4.1 Effect of load factor

Load factors are usually taken high enough to safely take care of any maneuver or gust load that might be encountered by the airplane during service. In the following we investigate the effect of the value of the design load factor (N_z) on the resulting optimum wing design. Six load factor values ranges from 1.0 to 6.0 with increment 1.0 were tried out. The maximum diving speed was kept at 108.0 m/s, and the flight altitude at 3.0 Km. The wing rigid twist was taken zero at all spanwise stations. Fig.3 shows variation of the optimum values of the aspect ratio, taper ratio and spar locations with the design load factor. It is seen that good wing designs should have smaller aspect ratios and taper ratios as the design load factor increases. The front spar location was seen to be shifted slightly towards the leading edge as the load factor increases. The same is applied to the rear spar but towards the trailing edge, which means that the enclosed cell area of the main wing box structure enlarges with the load factor. Fig.4 shows the optimum spanwise distribution of the front-spar flange area for the different selected values of the design load factor. It is seen that the increase in the load factor has a direct impact on increasing the cross sectional area of the spar-flange. Additional results have indicated that the load factor does not significantly affect the cross-sectional area of the rear-spar flange, where stresses were found to be much less than the allowable values. The optimum spanwise distributions of the front and rear shear web thicknesses for different values of the load factor are presented in Fig.5. As a general observation, the web thickness is directly proportional to the design load factor, which is a logical expected behavior. The front shear web thickness is recommended to have a faster rate of taper as the load factor increases.

5.4.2 Effect of diving speed

Fig.6 shows the variation of the optimum values of the aspect ratio, taper ratio and spar locations with the airplane maximum diving speed. It is seen that the optimum aspect ratio is slightly decreased as the design speed increases. On the other hand, the optimum taper ratio is remarked to be slightly increased with the design speed. Also, for good wing designs, the rear spar is recommended to be shifted backwards as the design speed increases, which results in a larger cell width. The optimum spanwise distribution for the front-spar flange area was found to vary in a small band bounded by the maximum speeds of 80 m/s and 110 m/s. No significant changes in the optimum rear-spar flange area, which was about 35% of that of the baseline design, were found when the maximum speed change through the prescribed interval (80-110) m/s. The optimal thickness distributions of the front and rear shear webs were seen to change within a very small interval ranges from 80 m/s to 110 m/s, where quick tapering was found to be recommended at low speeds.

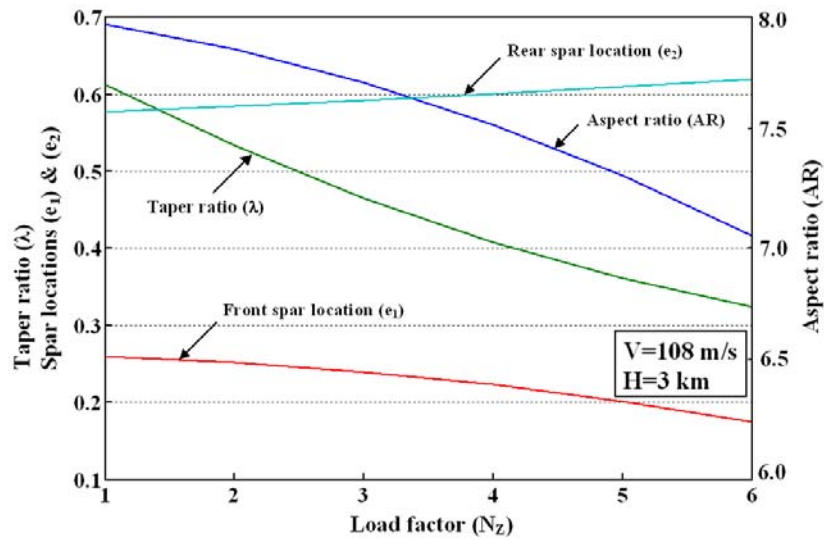


Fig. 3. Variation of optimum spar locations and planform configuration with load factor.

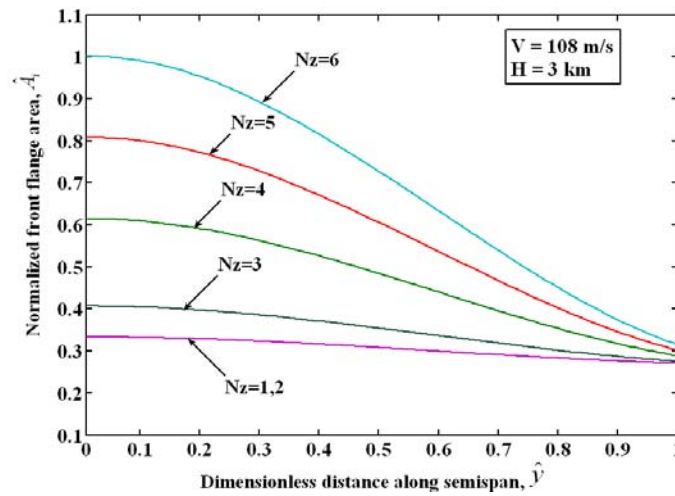
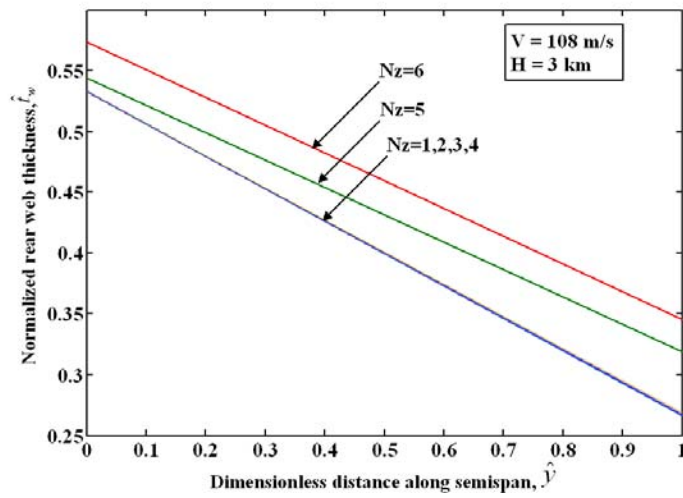
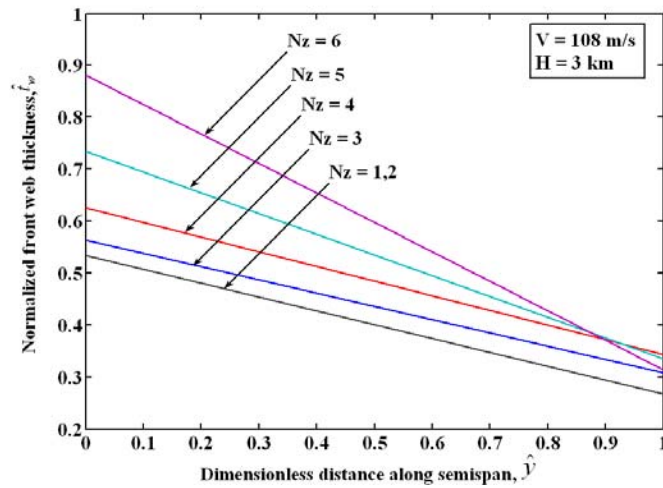


Fig. 4. Optimal front flange area distribution for different values of the design load factors.



(a) Rear shear web.



(b) Front shear web.

Fig. 5. Optimal web thickness distribution of wing spars for different load factors

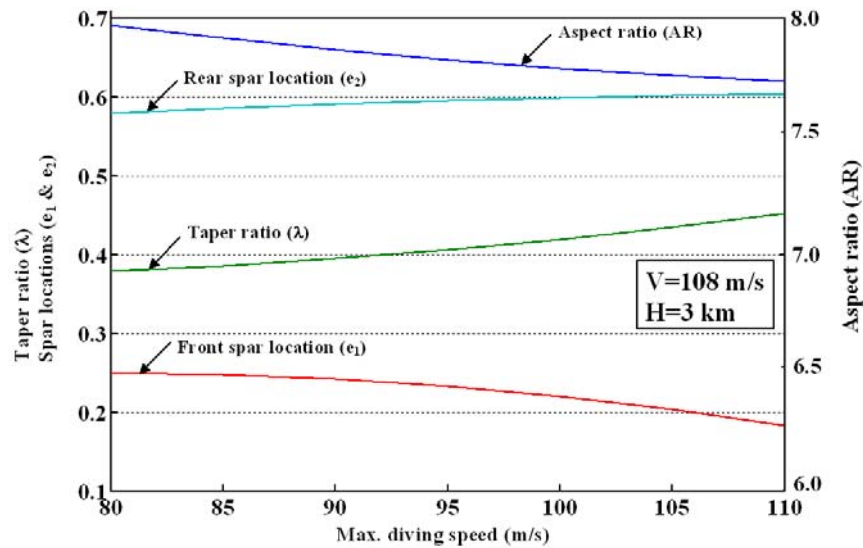


Fig. 6. Effect of speed variation on optimum planform configuration and spar locations.

6. Conclusions and Recommendations

In view of the importance of improving the aerodynamic and structural efficiencies of an airplane wing, an appropriate optimization model has been formulated and applied successfully to the wing of a low subsonic, light training airplane; namely, the AEIO-360A airplane for coast patrol. The main aspects of the wing design optimization, which reflects important design objectives, variables and constraints have been developed and identified. Four optimization strategies were considered and tested through extensive computer implementations. The first was based on minimizing the total weight of the main wing structure subject to strength, stiffness and aeroelastic constraints. The second strategy considered maximization of the critical flight speed at which divergence occurs, while the third one focused on minimization of the wing drag/lift ratio as a measure of improving aerodynamic efficiency. The last strategy, based on minimization of the power consumption, worked very well and has shown simultaneous balanced improvement in both of the aerodynamic and structural efficiencies. Design variables encompassed the wing aspect and taper ratios, spar locations, spar flange areas and web thicknesses, and skin thickness distributions. The optimization problem has been formulated as a nonlinear mathematical programming problem solved by the method of feasible directions. Conspicuous design trends have been obtained, showing variation of the optimum wing geometry and the cross-sectional variables for several flight conditions and specifications. The study presents detailed formulation of the general governing equations in the case of pull-out from a dive, where the continuous system was approximated by a finite discrete system along the wing span using the so-named Multhopps stations. Structural, aerodynamic and aeroelastic analyses assumed slender one-dimensional configuration. It makes use of the quasi-steady strip theory in evaluating aerodynamic loads and the classical engineering theories of bending and torsion in calculating stresses and deformations. Linearly elastic, isotropic and homogenous materials were postulated. Results have revealed that the approach implemented in this study can be efficient in producing improved designs in a reasonable computer time. In conclusion, an efficient design approach has been given by formulating an appropriate optimization model and implementing the *MATLab optimization Toolbox* routines coupled with the developed

structural and aeroelastic routines to find the needed optimal wing designs. Extension of this work would consider wing optimization against flutter and undesired vibrations. Other variables that need to be examined include the type of wing cross-section, type of material of construction, sweep and dihedral angles.

7. References

- [1] Ashley H., "On making things the best-aeronautical uses of optimization," *Journal of Aircraft*, Vol.19, No.1, 1982, pp. 5-28.
- [2] Edwin L., "Application of practical optimization techniques in the preliminary structural design of a forward-swept wing," *Second International Symposium on Aeroelasticity and Structural Dynamics*, Aachen, W. Germany, 1985.
- [3] Grossman B., Strauch G.J., Eppard W.M., Gurdal Z, and Haftka R.T., "Integrated aerodynamic/structural design of sailplane wing," *AIAA/AHS/ASEE, Aircraft Systems Design and Technology meeting Conference*, Dayton, OH, USA, October 1986.
- [4] Bulter R., Lillico M., Banerjee J.R. and Gum S., "Optimum design of high aspect ratio wing subject to aeroelastic constraints," *AIAA/ASME/ASCE/AHS, Structure, Structural Dynamics and Materials Conference*, New York, 1995, pp. 558-566.
- [5] Peter J.R., Dimitri N.M. and Daniel P.S., "Combined aerodynamic and structural optimization of a high-speed civil transport wing," *AIAA paper-95-1222*, 1995.
- [6] Negm H.M. and Maalawi K.Y., "A global objective function for aircraft design optimization," *Scientific Engineering Bulletin*, Cairo University, No.4, 1986, pp. 97-123.
- [7] Livine E., Schmit L.A. and Friedmann P.P., "Towards integrated multidisciplinary synthesis of actively controlled fiber composite wings," *Journal of Aircraft*, Vol. 27, No. 12, 1990, pp. 979-992.
- [8] Neill D.J., Johnson E.H. and Canfield R., "ASTROS – A Multidisciplinary Automated Structural Design Tool," *Journal of Aircraft*, Vol. 27, No. 12, 1990, pp. 1021-1027.
- [9] Papila M., Haftka R.T., Mason W.H. and Alves R., "Tailoring wing structures for reduced drag penalty in off-design flight conditions", *AIAA Journal* No, 4637, 2004.
- [10] Librescu L & Maalawi K., "Material grading for improved aeroelastic stability of composite wings", *Journal of Mechanics of Materials and Structures*, 2(7), pp. 1381-1394. 2007.
- [11] Librescu L. and Maalawi K.Y., "Aeroelastic design optimization of thin-walled subsonic wings against divergence," *Journal of Thin-Walled Structures*, 47, pp.89-97, 2009.
- [12] Bisplinghoff R.L. and Ashley H., "Principles of Aeroelasticity", John Wiley & Sons, Inc. New York, 1962.
- [13] Fox R.L., "Optimization methods for engineering design", Mass: Addison-Wesley, Reading, 1971.
- [14] Abbott I.H. and Von Doenhoff A.E., "Theory of Wing Sections", Dover Publication Inc., New York, 1958.
- [15] Bruhn E.F., "Analysis and Design of Flight Vehicle Structures", 1965.
- [16] Venkataraman P., "Applied optimization with MatLab programming", John Wiley & Sons, Inc., New York, 2002.